AD-A250 497

ATION PAGE

Form Approved OMB No 0704-0188

(2)

1. AGENCY USE ONLY

DATE

3. REPORT TYPE AND DATES COVERED
Final Report 01Dec89-30 Nov 91

4. TITLE AND SUBTITLE
Compact Millimeter wave devices: dielectric loaded carm, high voltage carm, slow wave crm and high harmonic gyrotron

5. FUNDING NUMBERS
AFOSR-90-0005

6. AUTHOR(S)

Dr Neville Luhmann, Jr

7. PERFORMING ORGANIZATION NAME(S) AND ADDRESS(ES)

University of California
405 Hilgard Avenue
Los Angeles, CA 90024

8. PERFORMING ORGANIZATION REPORT NUMBER

92 0380

9. SPONSORING/MONITORING AGENCY NAME(S) AND ADDRESS(ES)

AFOSR/NE
Bldg 410
Bolling AFB DC 20332-6448
Dr Barker

10. SPONSORING/MONITORING AGENCY REPORT NUMBER

2301/A8

11. SUPPLEMENTARY NOTES

12a. DISTRIBUTION/AVAILABILITY STATEMENT

UNLIMITED

12b. DISTRIBUTION CODE

13. ABSTRACT (Maximum 200 words)

A gyro-BWO can provide broardband slow timescale tunability by adjusting the magnetic field and fast narrowband tunability by varying the gun's voltage. This device depends on the internal feedback of the fast wave interaction between the electro beam's cyclotron resonance wave and a backward electromagnetic wave. Although the previous two experiments were operated at kW power levels, a gyro-BWO is capable of much higher power. (See report for more detail).

14. SUBJECT TERMS

15. NUMBER OF PAGES

16. PRICE CODE

17. SECURITY CLASSIFICATION OF REPORT	18. SECURITY CLASSIFICATION OF THIS PAGE	19. SECURITY CLASSIFICATION OF ABSTRACT	20. LIMITATION OF ABSTRACT
UNCLASSIFIED	UNCLASSIFIED	UNCLASSIFIED	UL

RESEARCH SUMMARY

PROJECT TITLE:
"Compact Millimeter-Wave Devices: Dielectric Loaded carm, high voltage carm, slow wave crm and high harmonic gyrotron

CONTRACT/GRANT NO.:
90-0005

CONTRACT/GRANT VALUE:
$99,732

CONTRACT/GRANT PERIOD OF PERFORMANCE:
Dec. 1, 19[illegible] - Nov. 30, 1991

PRINCIPAL INVESTIGATOR:
N.C. Luhmann, Jr.

TELEPHONE NO.:
(310) 825-4163

BUSINESS MAILING ADDRESS:
UCLA, Electrical Engineering Department
63-143 Engineering IV
Los Angeles, CA 90024

RESEARCH OBJECTIVES:
Basic research studies on the generation of high frequency waves at high power while minimizing problematic technological requirements such as high voltage and intense magnetic fields.

AFOSR PROGRAM MANAGER:
Dr. Robert Barker

APPROACH

During the last grant period, a unique mm-wave rf component and four interactions for mm-wave generation were under development. (1) We are constructing a 100 kW, tunable 60 GHz gyro-BWO, which will generate an output power nearly two orders of magnitude higher than any previous gyro-BWO. The 1 MW MIG electron gun was removed from a 200 kW, 60 GHz Varian gyrotron. Our gyro-BWO will depend on the fast wave interaction between the electron beam's cyclotron resonance wave and a backward TE_{01} cylindrical waveguide mode.

(2) We have begun to develop a high harmonic peniotron travelling-wave amplifier, which is predicted to be extremely efficient because all electrons lose energy in the interaction. The axis-encircling electrons will rotate within a magnetron-type waveguide.

(3) Using a dielectric loaded waveguide, a gyro-TWT amplifier can be designed with a very wide bandwidth. Whereas a conventional gyro-TWT has an instantaneous bandwidth of only several percent, the dielectric loaded gyro-TWT has been shown to yield an instantaneous bandwidth of 20% due to the dielectric's reduction of the waveguide's dispersion.

(4) We are also developing a frequency selective cavity in which these interactions can be realized as oscillators. In a Bragg resonator, the two reflectors consist of corrugated waveguide. A wave which satisfies the Bragg condition, $\lambda_{||} = 2\ell$, where $\lambda_{||}$ is the axial wavelength and ℓ is the corrugation period, is reflected through the principle of constructive interference.

(5) In addition, we are developing a novel, efficient, high power microwave source, the Negative Energy Cyclotron Resonance Maser, which depends on the coupling of the negative energy cyclotron wave to a positive energy slow waveguide mode, just as a conventional TWT is based on a negative energy space charge wave. Since the beam mode is a negative energy wave, an initial transverse velocity is not required for wave growth. Thus, it is straightforward to create the device's electron beam. We have suggested utilizing the same dielectric loaded slow wave structure as in (3) above, and to provide frequency selective feedback to favor the growth of the cyclotron wave over the competing space-charge wave by corrugating the dielectric into a Bragg reflector as discussed in (4) above.

PROGRESS (Dec. 1, 1990 - Nov. 30, 1991)

1. Gyro-BWO

A gyro-BWO can provide broadband slow timescale tunability by adjusting the magnetic field and fast narrowband tunability by varying the gun's voltage. This device depends on the internal feedback of the fast wave interaction between the electron beam's cyclotron resonance wave and a backward electromagnetic wave. Although the previous two experiments were operated at kW power levels, a gyro-BWO is capable of much higher power.

We have finished the construction of a high power reflection-type gyro-BWO, utilizing a 60 GHz Varian gyrotron MIG and a superconducting solenoid with a uniform length of 5 cm obtained from Hughes Aircraft. The parameters are given in Table 1. To achieve continuous frequency tuning, the wall of the interaction tube has been severed with three slices separated in azimuth by 120° as shown in Fig. 1 to destroy modes without a threefold azimuthal symmetry. A self-consistent slow timescale simulation code has been obtained from Dr. Caplan of LLNL and used to model the device. The power in the linearly polarized

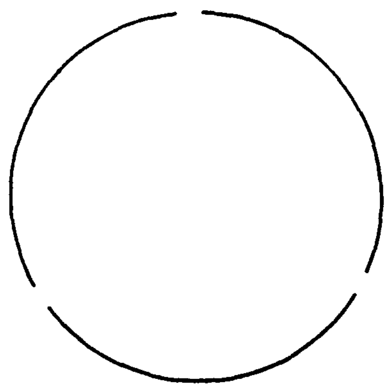

Figure 1. Schematic of interaction circuit which has been severed thrice to suppress all modes without a third order azimuthal symmetry.

Table 1. Parameters of Gyro-BWO.

Beam Voltage	75 kV
Beam Current	10 A
Power	10-60 kW
Frequency	46-63 GHz
Magnetic Field	20-30 kG
α	1.5
$\Delta v_z/v_z$	5%
Mode	TE_{31}
r_{gc}/r_w	0.5
Circuit Radius	0.454 cm
Circuit Length	6 cm

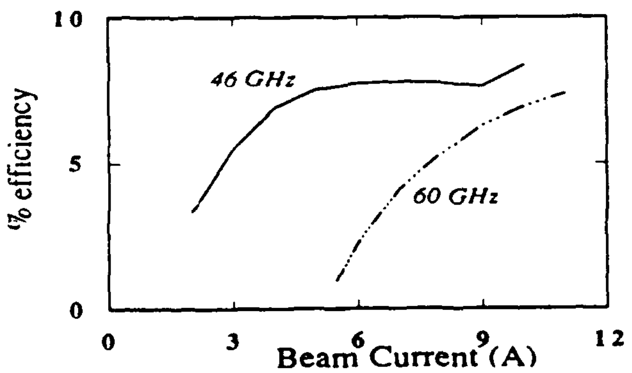

Figure 2. Dependence of efficiency at 46 and 60 GHz on beam current for an interaction length of 6 cm ($\Delta v_z/v_z = 0\%$).

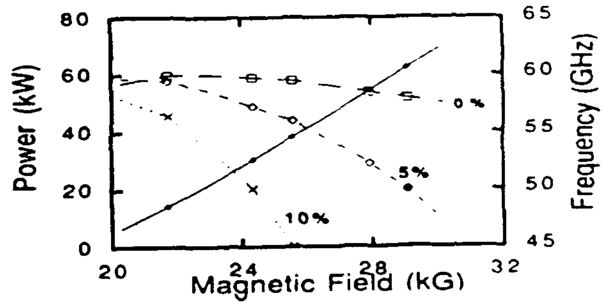

Figure 3. Dependence of power and frequency on magnetic field for a beam current of 10 A, an interaction length of 6 cm and axial velocity spreads of 0%, 5% and 10%.

TE_{31} mode is shown in Fig. 2 as a function of beam current. The starting current at 46 GHz is 6 A. Figure 3 shows the predicted tunability of the device for several values of velocity spread. A frequency tuning range of 30% can be achieved by varying the magnetic field by 50%. For an axial velocity spread of 5%, the output power is predicted to vary from 40-60 kW and the efficiency varies from 8-12%.

The experiment has been constructed. Only minor tasks remain, such as repairing vacuum leaks. A large vacuum chamber to enclose the experimental components has been prepared. The slotted gyro-BWO interaction tube has been fabricated. Lossy rings have been obtained to keep the electron beam from oscillating before it reaches the BWO circuit. A 100 kV modulator to provide the cathode voltage has been assembled and tested. A voltage divider for the mod-anode voltage has been obtained from Hughes. The solenoid has successfully been made to go superconducting. The experiment should begin within two months.

2. High Harmonic Peniotron

We have begun to plan and assemble a third harmonic penio-TWT experiment. The peniotron is of much interest because it can yield an efficiency of nearly 100%. The resonance condition for a high harmonic peniotron with an axis-encircling electron beam interacting with a TE_{n1} mode is $\omega = (n-1)\Omega_c$ (compare to $\omega = n\Omega_c$ for the gyrotron). In a peniotron, the electrons advance by one cycle in the wave as they complete one gyro-orbit. Due to the asynchronous condition, the electrons effectively experience the TE_{n1} wave as a plane wave, resulting in an $\underline{E} \times \underline{B}$ drift of each guiding center toward the azimuth where it is phased to lose energy and because the field has a strong gradient, on the average it loses energy per period. The reason for the device's high efficiency is that all electrons lose energy. The ideal geometry for a high harmonic peniotron is the magnetron type cavity shown in Fig. 4. Since the vane structure determines the azimuthal symmetry of the allowed cavity modes, mode competition is greatly reduced. Also, the magnetron geometry greatly ameliorates the electron energy requirement, since it can be designed for any voltage electron beam. The ideal electron gun for this interaction is a cusp gun. However, they need further development before they are able to produce the high quality beams necessary for the TWT.

For our proof-of-principal experiment, we will use a gyroresonant rf accelerator to create the requisite axis-encircling beam. As used in our previous AFOSR-funded experiments where beam energies of $\approx$ 200-300 keV were employed and the beam currents were $\leq$ 1 A. By overcoupling the accelerator cavity, it appears relatively straightforward to produce 50-100 keV beams at current levels in the 5-20 A range. It was found in our measurements that the axial velocity spread of these beams is very low ($\Delta v_z/v_z < 2\%$).

During the last year, we have used a nonlinear self-consistent simulation code similar to that of Dr. Ganguly of NRL to investigate the high harmonic peniomagnetron-TWT. An initial study yielded the preliminary design for the third harmonic device characterized by Figs. 5 and 6 and summarized in Table 2. The spatial growth of power in the device is shown in Fig. 5 and Fig. 6 shows the expected bandwidth of 5%. Notice that the efficiency is a remarkable 50%.

The proposed interaction circuit for the high harmonic transmission type penio-TWT as presently envisioned would begin and end with a coupler to transform the fundamental TE_{10} mode of rectangular waveguide into the quasi-TE_{41} π-mode of the corrugated interaction waveguide with 8 vanes. We have begun to design the couplers for this TWT. For the

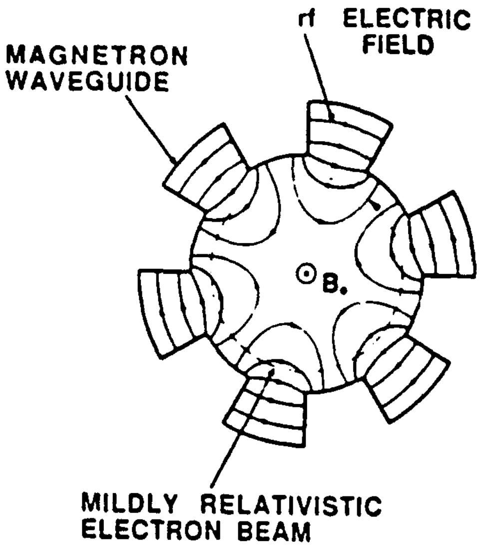

Figure 4. Cross-section of peniomagnetron cavity, where the rf electric field lines of the π mode are shown.

Table 2. Parameters of 35 GHz 3rd harmonic peniomagnetron-TWT amplifier.

Voltage	100 kV
Current	5 A
Peak Power	250 kW
Efficiency	50%
Gain	40 dB
Bandwidth	5%
Magnetic Field	4.5 kG
Vane Number	8
α	2.0
Electron Larmor Radius	0.218 cm
Inner Vane Radius	0.272 cm
Outer Vane Radius	0.412 cm
Interaction Length	14.5 cm

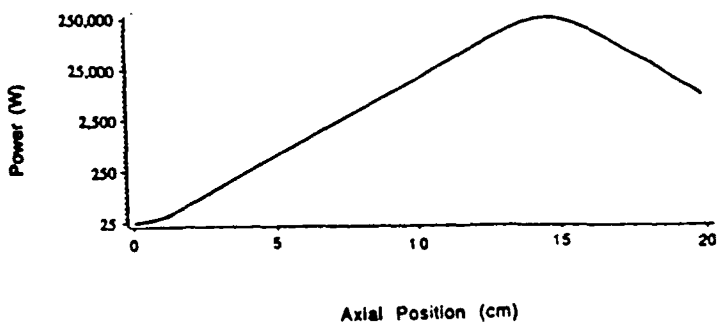

Figure 5. Spatial evolution of 35 GHz wave in peniomagnetron-TWT described in Table 2.

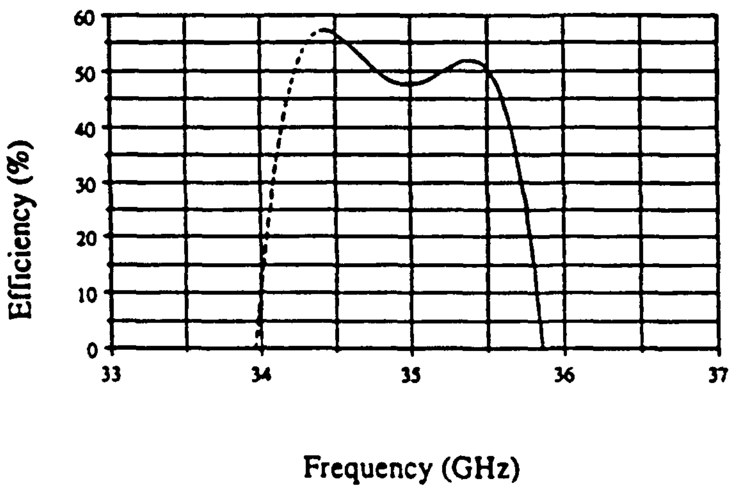

Figure 6. Predicted bandwidth of Ka-band peniomagnetron-TWT described in Table 2 ($V = 100kV$, $I = 5A$, $P_{out} \sim 250$ kW).

low power input coupler, we will modify the azimuthal phase velocity coupler from our eighth harmonic, smooth wall gyro-TWT coupler. In this design, the input fundamental rectangular waveguide is wrapped around the interaction tube with approximately six holes coupling the two together. The two structures are chosen so that the wavelength of the input wave in the rectangular waveguide is equal to the azimuthal wavelength of the desired magnetron mode. The resulting coupling is then constructive. The wave is launched in the desired direction by placing a radial discontinuity (an effective shorting plate) in the tube in the other direction and separated from the coupling hole by an odd number of quarter-wavelengths. Since the electromagnetic energy at the far end of the vanes is magnetic, the coupling must also be magnetic. We will couple to the magnetron's magnetic field from the rectangular waveguide's magnetic field through an array of slits.

The high power output coupler will be a mode converter as used in ECR heating of Fusion Tokamaks. By using a periodically corrugated tube the TE_{41} mode in circular waveguide can be converted into the TE_{11} mode if the corrugation has a m=5 azimuthal symmetry and if the axial period corresponds to the beat period of the two waves ($\ell = \lambda_1\lambda_2/(\lambda_1 - \lambda_2)$, where λ_i represents the axial wavelength of the two waves). We have continued our collaboration with Drs. Thumm and Pretterebner of Stuttgart University, who had earlier designed our Hamming-Window Bragg reflectors and who have now designed a broadband TE_{41}/TE_{11} converter. Figure 7 shows the transfer of energy from the TE_{41} mode to the TE_{11} mode in the tapered two period converter and Fig. 8 shows the converters bandwidth, which is greater than the bandwidth of the peniotron as required.

3. Bragg Reflectors

A Bragg resonator is the most suitable cavity structure for providing frequency selective feedback for overmoded, high power oscillators such as CARMs and FELs. Two Bragg resonators were formed by separating two reflector sections by a smooth uncorrugated aluminum tube of length L_R. Each set was described in the previous progress report. One set used our sinusoidal corrugation reflectors and the other used two dissimilar Hamming-Window Bragg reflectors. The inner radius of the smooth central section is equal to the minimum inner radius of the corrugation for both resonators. The transmission method has been used to measure the resonant frequency and Q of the modes in both cavities. The signal was coupled in and out through ports on the sidewall of the smooth resonator section.

The transmission method measures the loaded Q of the resonating systems given by

$$\frac{1}{Q_L} = \frac{1}{Q_{Bragg}} + \frac{1}{Q_{ohmic}} + \frac{1}{Q_{ext}} \qquad (1)$$

In order to directly measure the diffraction Q of the Bragg cavity, Q_{ext} must be large compared to Q_{Bragg}. The values of Q_{ext} can be adjusted by decreasing the coupling strength of the sidewall coupling port such that

$$Q_{ext} \gg Q_{Bragg} \qquad (2)$$

Then, the effective loaded Q of the resonator, neglecting Q_{ext}, is given by

$$\frac{1}{Q'_{Bragg}} = \frac{1}{Q_{Bragg}} + \frac{1}{Q_{Ohmic}} \qquad (3)$$

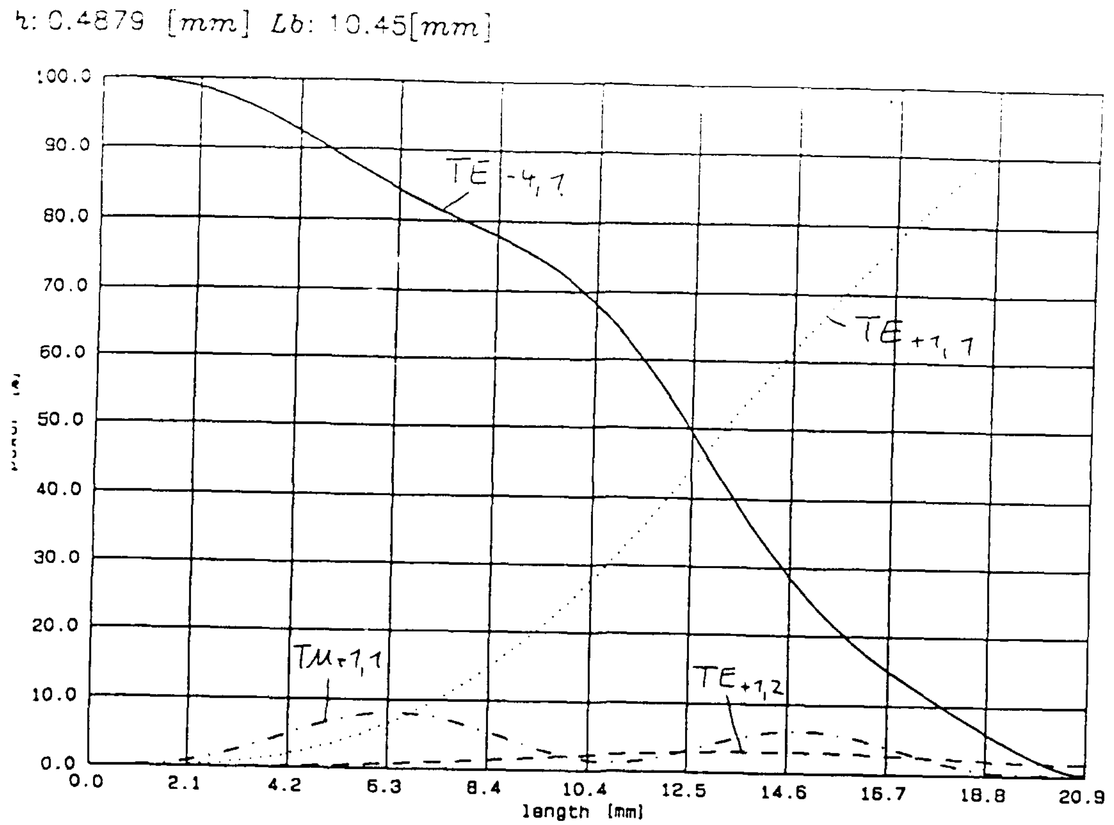

Figure 7. Spatial dependence of power conversion of 95 GHz wave from TE_{41} mode to TE_{11} mode and other spurious modes in the tapered two beat period TE_{41}/TE_{11} converter. (Note: converter can be trivially scaled to other frequencies by scaling the dimensions of the converter).

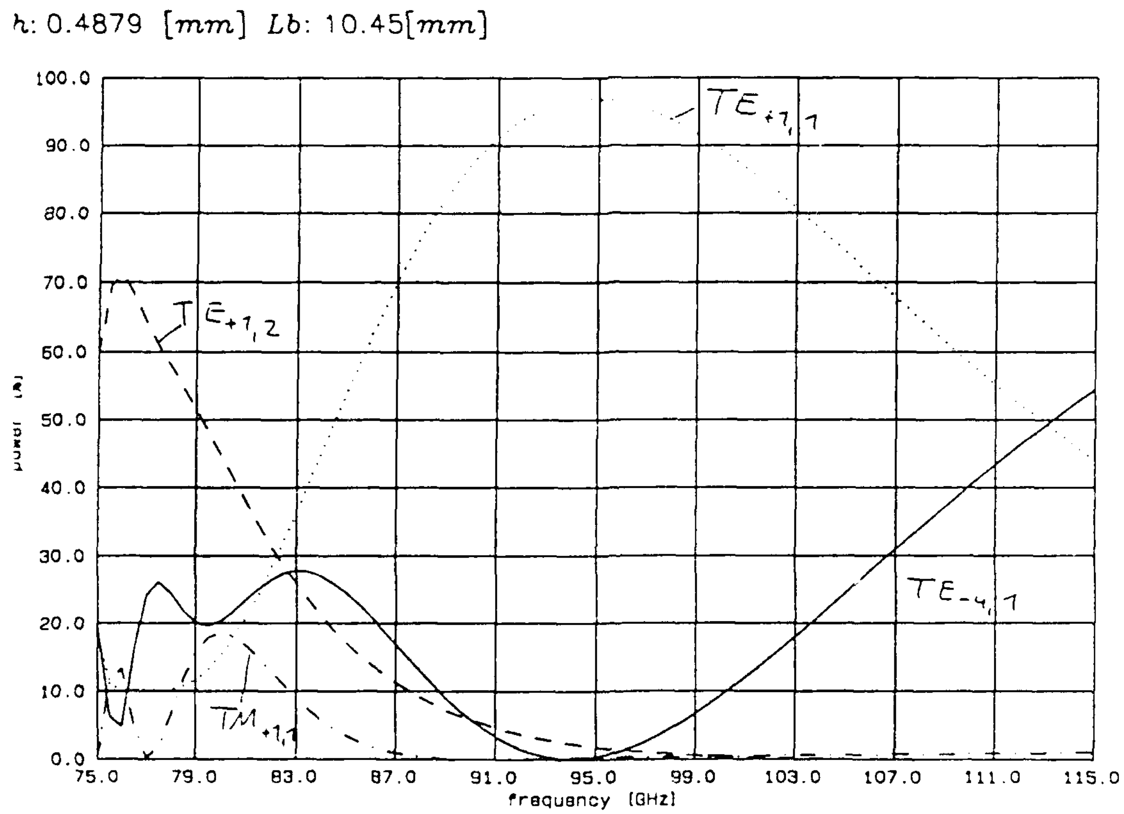

Figure 8. Bandwidth of conversion efficiency from TE_{41} mode into TE_{11} mode in tapered two-period TE_{41}/TE_{11} converter.

Both the experimental and theoretical values of Q'_{Bragg} have been found over the bandwidth of the sinusoidal corrugation Bragg reflector by changing the length of the smooth section of the resonator, thereby changing the resonant frequency of the mode. The measurements of Q'_{Bragg} are shown in Fig. 9 along with the theoretical predictions from the eigenvalue/eigenvector method, which includes Ohmic losses equal to twice the theoretical value, and the qualitative approximation

$$Q = (w/c)^2 L_R/[k(1 - R_1 R_2)] \tag{4}$$

where $R_1$and R_2 are the reflectivity (in amplitude) of the two corrugated sections and k is the free space propagation constant. The experimental bandwidth for Q is broader than the theoretical prediction as was the experimental bandwidth for reflectivity.

The measured Q'_{Bragg} of the resonator with Hamming-Window Bragg reflectors is shown in Fig. 10 along with the qualitative approximation (Eq. 4) using the reflectivity predicted by Stuttgart's scattering matrix code. The measured Q over the bandwidth is in good agreement with the theoretical prediction. Considering the sensitivity of Eq. 4 on $1/(1-|R_1||R_2|)$ for $|R_1||R_2| \approx 0.95$, the small discrepancy in the Q values is quite reasonable.

4. Wideband Gyro-TWT

The development of the Dielectric Loaded Broadband Gyro-TWT with a predicted bandwidth of 20% has continued. This device achieves wideband amplification because the interaction waveguide is loaded with dielectric to reduce its dispersion so that the group velocity of the waves is essentially constant over a fairly wide frequency range. The construction of the device is well underway. The single anode MIG electron gun has been ordered. The 100 kV modulator has been successfully tested. A 4 kG copper solenoid with a high magnetic uniformity (± 0.3%) over a length of 1 m has been ordered with funds from another agency. The dispersion of the rectangular waveguide with dielectric slabs along the two narrow walls has been measured. Figure 11 compares the experimental measurements with the dispersion predicted by analytical theory.

5. Negative Energy CRM

In addition, we have begun the development of components for an exciting new device which we had investigated theoretically during the previous year. In the negative energy cyclotron resonance maser, a negative energy cyclotron wave is coupled to a positive energy, slow waveguide mode. This concept is similar to that exploited in conventional TWTs, where a negative energy space-charge wave is coupled to a positive energy, slow waveguide mode. The resonance condition of the negative energy wave is $\omega = -\Omega_c + k_{||}v_{||}$ (to be compared with the resonance condition of the usual cyclotron resonance maser (CRM), which is $\omega = \Omega_c + k_{||}v_{||}$). Whereas the conventional CRM requires an electron beam with a significant transverse velocity for wave growth, the negative energy CRM uses a beam with a purely axial velocity. The free energy for wave growth derives from the electron

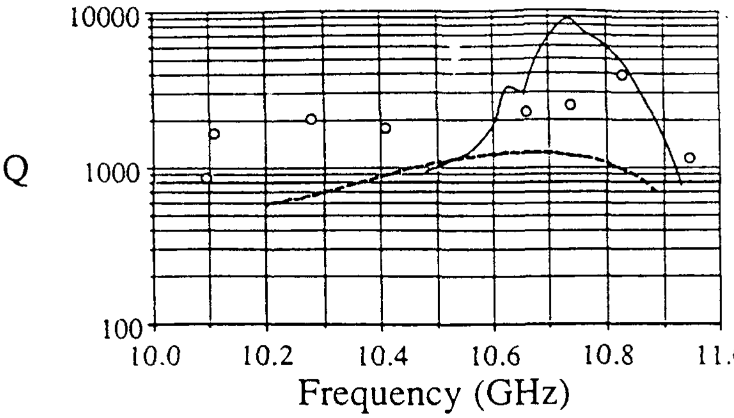

Figure 9. Theoretical dependence of a sinusoidal Bragg resonator's quality factor on frequency from measurement (open circles), the eigenvalue/eigenvector method (solid line) and from Eq. 4 (dashed line).

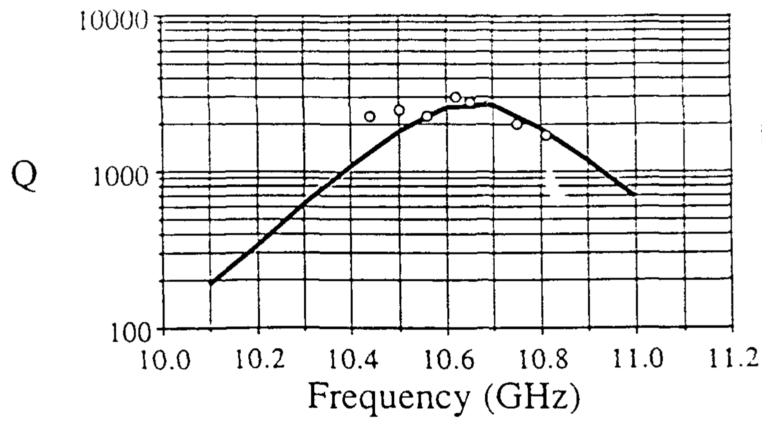

Figure 10. Theoretical dependence of a Hamming-Window Bragg resonator's quality factor on frequency from measurement (open circles) and Eq. 4 (solid

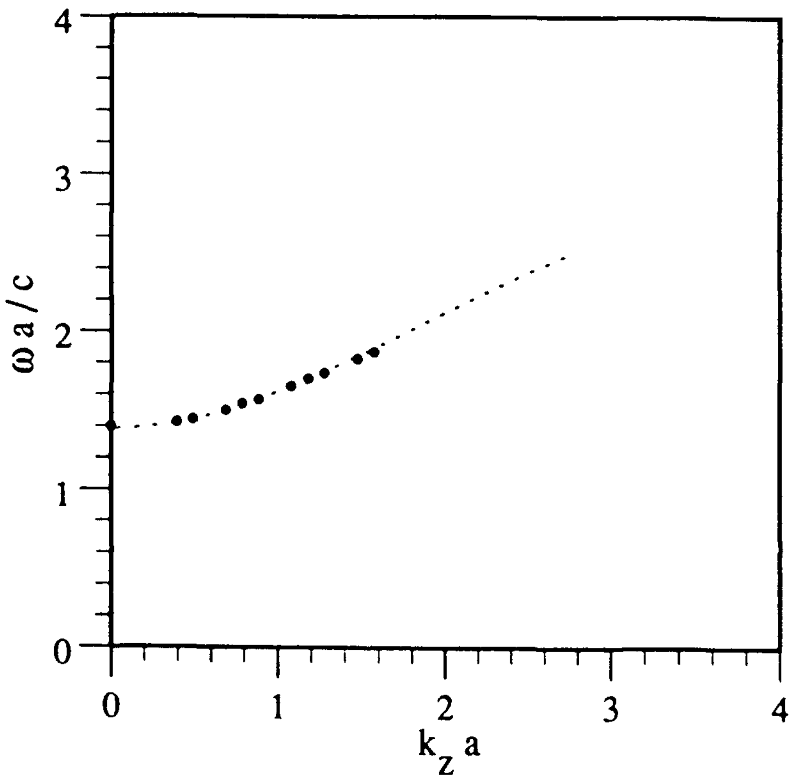

Figure 11. Measured frequency versus propagation constant of lowest order LSE_{10} modes in dielectric loaded waveguide compared to theoretical values.

beam's streaming motion. For intense ($\omega_p/\omega \geq 0.1$), high voltage ($\gamma \geq 2$) electron beams, the growth rate of this interaction can be even stronger than for the space charge mode and the efficiency can be very high (20-30%).

We propose to test this interaction using our 350 kV SLAC 5045 Klystron electron gun and our SLAC-style 400 kV modulator. Our interaction waveguide will be the same dielectric loaded rectangular waveguide as will be used in our Dielectric-Loaded Wideband Gyro-TWT (see Sec. 4 above). To further enhance the growth of the cyclotron wave over the space charge wave, we have built a dielectric Bragg reflector designed to provide feedback at the frequency of the cyclotron wave. The dielectric Bragg reflector is currently being measured.

PUBLICATIONS AND PRESENTATIONS (Dec. 1, 1990 - Nov. 30, 1991)

"CARM Amplifier Designs for High Power," Q.S. Wang, D.B. McDermott, A.T. Lin, N.C. Luhmann, Jr., K.R. Chu, A. Salop and M. Caplan, *Int. J. of Infrared and Millimeter Waves* 12, 297 (1991).

"Dielectric Loaded Wideband Gyro-TWT," K.C. Leou, D.B. McDermott and N.C. Luhmann, Jr., accepted for publication, *IEEE Trans. on Plasma Science.*

"Bragg Reflectors," C.K. Chong, D.B. McDermott, M.M. Razeghi, N.C. Luhmann, Jr., J. Pretterebner, D. Wagner, M. Thumm, M. Caplan and B. Kulke, accepted for publication, *IEEE Trans. on Plasma Science.*

"Negative Energy Cyclotron Resonance Maser," E.E. Lednum, D.B. McDermott, A.T. Lin and N.C. Luhmann, Jr., *1990 Int. Electron Devices Meeting*, San Francisco, California, 1990.

"Dielectric Loaded Broadband Gyro-TWT," K.C. Leou, D.B. McDermott and N.C. Luhmann, Jr., *1990 Int. Electron Devices Meeting*, San Francisco, California, 1990.

"Bragg Reflectors: Tapered and Untapered," C.K. Chong, M.M. Razeghi, D.B. McDermott, N.C. Luhmann, Jr., M. Thumm and J. Pretterebner, *1991 SPIE Conf. on Beams and High Power Microwaves*, Los Angeles, California, 1991.

"Magnetically Tapered CARM for High Power," Q.S. Wang, D.B. McDermott and N.C. Luhmann, Jr., *1991 SPIE Conf. on Beams and High Power Microwaves*, Los Angeles, California, 1991.

"Negative Energy Cyclotron Resonance Maser," E.E. Lednum, D.B. McDermott, A.T. Lin and N.C. Luhmann, Jr., *1991 SPIE Conf. on Beams and High Power Microwaves*, Los Angeles, California, 1991.

"100 kW, 46-63 GHz Severed Gyro-BWO," G. Vasilakos, T.R. Stephenson, G.D. Ramlow, D.B. McDermott, N.C. Luhmann, Jr., and M. Caplan, *16th Int. Conf. on Infrared and Millimeter Waves*, Lausanne, Switzerland, 1991.

"Bragg Reflectors with Hamming-Window Taper," D.B. McDermott, C.K. Chong, N.C. Luhmann, Jr., M. Thumm, and J. Pretterebner, *1991 APS Plasma Physics Meeting*, Tampa, FL, 1991.

"Dielectric-Loaded Wideband Gyro-TWT," K.C. Leou, D.B. McDermott and N.C. Luhmann, Jr., *1991 APS Plasma Physics Meeting*, Tampa, FL, 1991.

"100 kW, 46-63 GHz Gyro-BWO," G. Vasilakos, T.R. Stephenson, G.D. Ramlow, D.B. McDermott, and N.C. Luhmann, Jr., *1991 APS Plasma Physics Meeting*, Tampa, FL, 1991.

"Unique Gyro-TWTs at UCLA," Q.S. Wang, C.K. Chong, K.C. Leou, C.S. Kou, D.B. McDermott, and N.C. Luhmann, Jr., submitted to *1992 Microwave Power Tube Conference.*

"Fast-Wave Research at UCLA," T.S. Stephenson, J.D. McNally, G. Vasilakos, M.P. Bobys, Q.S. Wang, C.K. Chong, K.C. Leou, D.B. McDermott, and N.C. Luhmann, Jr., submitted to *1992 Microwave Power Tube Conference.*